Structure of Perfect Tracking Controller Based on Multirate Feedforward Control

Hiroshi Fujimoto*, Yoichi Hori*, and Atsuo Kawamura**

Department of Electrical Engineering, The University of Tokyo*
7-3-1 Hongo, Bunkyo, Tokyo, 113-8656, Japan
Phone: +81-3-5841-7683, Fax: +81-3-5841-7687
E-Mail: fuji@hori.t.u-tokyo.ac.jp

Yokohama National University, Japan**

Abstract

In this paper, a novel perfect tracking control method based on the multirate feedforward control is proposed. Moreover, by generalizing the relationship between the sampling period of the plant output and the control period of the plant input, the proposed method can be applied to various systems with hardware restrictions of these periods, and achieve higher performance. Next, it is shown that the structure of the proposed perfect tracking controller is very simple and clear. Illustrative examples of position control using a dc servo motor are presented, and simulations and experiments demonstrate the advantages of this approach.

Key words: Digital control, motion control, multirate sampling control, two-degree-of-freedom, tracking control

1   Introduction

In the digital motion control system, the tracking controllers are often employed for high speed and high precision servo systems because the controlled plant follows the smoothed desired trajectory. The best tracking controller is ideally the Perfect Tracking Controller (PTC) which controls the controlled object with zero tracking error [1]. The perfect tracking can be achieved using the feedforward controller $C_1[z]$ which is realized by the inverse system of the closed-loop system $G_{cl}[z]$.

$$C_1[z] = \frac{1}{z^d G_{cl}[z]} \tag{1}$$

where d is the relative degree of $G_{cl}[z]$.

However, the discrete-time plant discretized by the zero-order-hold usually has unstable zeros [2]. Thus, $C_1[z]$ becomes unstable because $G_{cl}[z]$ has the unstable zeros. Therefore, in the conventional digital control systems utilizing the zero-order-holds, the perfect tracking is usually impossible.

From this viewpoint, two feedforward control methods are proposed for the discrete-time plant with unstable zeros in [1]. First, the Stable Pole Zero Canceling (SPZC) controller cancels all poles and stable zeros of the closed-loop system, which has both phase and gain errors caused by the uncancellable unstable zeros. Second, Zero Phase Error Tracking Controller (ZPETC) adds the factors which cancel the phase error to SPZC. However, the gain error caused by the unstable zeros remains. Moreover, [3], [4], and [5] have attempted to compensate for the gain error of ZPETC. However, these methods are not able to realize the perfect tracking because the zero-order-holds are employed.

Authors have proposed a novel perfect tracking control method using multirate feedforward control instead of the zero-order-hold [6]. On the other hand, a lot of industrial systems often have hardware restrictions both on the sampling periods to detect plant outputs and the control periods to generate plant inputs. For example, in head-positioning control of hard disk drives and visual servo systems, the sampling periods of the plant output should be longer, because the servo signals and video signals are detected at slower periods than the control inputs. In contrast, systems with low speed D/A converters or CPUs have restrictions that the periods of the plant inputs are slower than the sampling periods of the plant outputs. In this paper, the perfect tracking control is extended to be applied to various systems with such hardware restrictions by generalizing the output sampling period. Next, it is shown that the structure of the proposed controller is very simple and clear.

The unstable zeros problems of the discrete-time plant have been resolved by zero assignment in use of multirate control [7, 8]. However, [9] shows that those methods have disadvantages of large overshoot and oscillation in the inter-sample points because the control input changes back and forth very quickly. On the other hand, the proposed method never has this problem because all of the plant states (e.g. position and velocity) are controlled along the smoothed desired trajectories.

2   Generalizations of the sampling periods

A digital tracking control system usually has two samplers for the reference signal $r(t)$ and the output
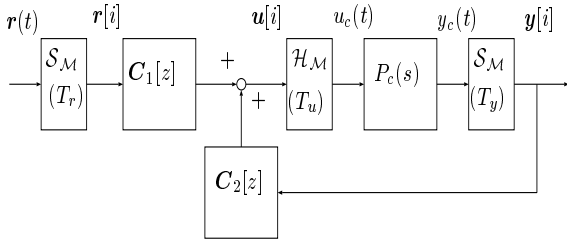
Figure 1. Two-degree-of-freedom control system.

(a) Case 1 $(T_y \leq T_u)$ (b) Case 2 $(T_y > T_u)$
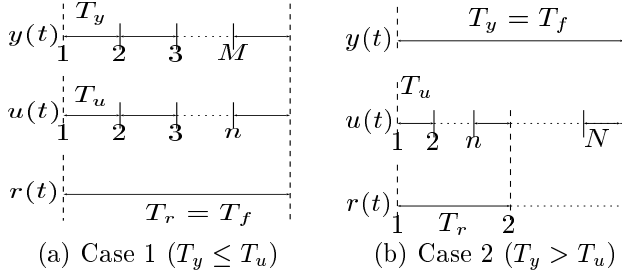
Figure 2. Multirate sampling control.

Figure 3. Generalized multirate sampling control.

$y(t)$, and one holder on the input $u(t)$ as shown in Fig. 1. Therefore, there exist three time periods T_r, T_y, and T_u which represent the period of $r(t), y(t)$, and $u(t)$, respectively. The input period T_u is generally decided by the speed of the actuator, D/A converter, or the calculation on the CPU. Moreover, the output period T_y is also determined by the speed of the sensor or the A/D converter.

Actual control systems usually hold the restrictions on T_u and/or T_y. Thus, the conventional digital control systems make these three periods equal to the longer period between T_u and T_y.

On the other hand, authors showed that the perfect tracking can be achieved on every sampling point T_r by letting $T_r = nT_u$, where n is the plant order [6]. In the following discussions, $T_r = nT_u$ is regarded as the condition for the perfect tracking. Moreover, the following two cases are considered, which are very ordinary in industries. First, although T_u is decided in advance by the hardware restrictions, the plant output can be detected at same or faster period $(T_y \geq T_u)$, as shown in Fig. 2(a). This case is referred to as case 1 in this paper, which includes usual servo systems of $T_y = T_u$ without special hardware restrictions. Second, although T_y is decided in advance, the plant input can be changed N times during T_y, as shown in Fig. 2(b). This case is also referred to as case 2, which includes systems with special hardware restrictions such as hard disk drives [10], visual servo systems, and servo systems with low precision encoder. In this case, the perfect tracking can be assured $N/n(\triangleq L)$ times during inter-sample points of T_y.

For the above multi-period systems, the longer period between T_r and T_y is defined as the flame period T_f [11]. Moreover, z-operator is also defined as $z \triangleq e^{sT_f}$. By using these definitions, case 1 and 2 can be dealt with together in the following discussions. The positive integers M and N are input and output multiplicities during T_f, respectively. In this paper, N have to be selected so that $N/n(= L)$ becomes an integer.

3   Designs of the proposed controller

In this section, the proposed perfect tracking control method is presented. For simplification, the plant is assumed to be SISO system. The proposed method, however, can be extended to deal with the MIMO system by the same way as [12].

3.1   Plant Discretization and Parameterization

In order to deal with cases 1 and 2 together, the multirate control scheme is represented by Fig. 3 in use of input and output multiplicities N and M. Thus, in case 1, N should be set to n. Moreover, in case 2, M also have to be set to 1.

Consider the continuous-time nth order plant $P_c(s)$ described by

$$\dot{\boldsymbol{x}}(t) = \boldsymbol{A}_c\boldsymbol{x}(t) + \boldsymbol{b}_c u(t) \ , \quad y(t) = \boldsymbol{c}_c\boldsymbol{x}(t). \quad (2)$$

The discrete-time plant $\boldsymbol{P}[z]$ discretized by the generalized multirate sampling control (Fig. 3) becomes

$$\boldsymbol{x}[i+1] = \boldsymbol{A}\boldsymbol{x}[i] + \boldsymbol{B}\boldsymbol{u}[i], \quad (3)$$
$$\boldsymbol{y}[i] = \boldsymbol{C}\boldsymbol{x}[i] + \boldsymbol{D}\boldsymbol{u}[i], \quad (4)$$

where $\boldsymbol{x}[i] = \boldsymbol{x}(iT)$, and where matrices $\boldsymbol{A}, \boldsymbol{B}, \boldsymbol{C}, \boldsymbol{D}$ and vectors $\boldsymbol{u}, \boldsymbol{y}$ are given by

$$\left[\begin{array}{c|c} \boldsymbol{A} & \boldsymbol{B} \\ \hline \boldsymbol{C} & \boldsymbol{D} \end{array}\right] \triangleq \left[\begin{array}{c|ccc} e^{\boldsymbol{A}_c T_f} & \boldsymbol{b}_1 & \cdots & \boldsymbol{b}_N \\ \hline \boldsymbol{c}_1 & d_{11} & \cdots & d_{1N} \\ \vdots & \vdots & & \vdots \\ \boldsymbol{c}_M & d_{M1} & \cdots & d_{MN} \end{array}\right], \quad (5)$$

$$\boldsymbol{u} \triangleq [u_1, \cdots, u_N]^T, \ \boldsymbol{y} \triangleq [y_1, \cdots, y_M]^T, \quad (6)$$

$$\boldsymbol{b}_j \triangleq \int_{(1-\mu_j)T_f}^{(1-\mu_{(j-1)})T_f} e^{\boldsymbol{A}_c \tau} \boldsymbol{b}_c d\tau \ , \ \ \boldsymbol{c}_k \triangleq \boldsymbol{c}_c e^{\boldsymbol{A}_c \nu_k T_f}, \qquad (7)$$

$$d_{kj} \triangleq \begin{cases} \mu_j < \nu_k : & \boldsymbol{c}_c \int_{(\nu_k - \mu_j)T_f}^{(\nu_k - \mu_{(j-1)})T_f} e^{\boldsymbol{A}_c \tau} \boldsymbol{b}_c d\tau \\ \mu_{(j-1)} < \nu_k \le \mu_j : & \boldsymbol{c}_c \int_0^{(\nu_k - \mu_{(j-1)})T_f} e^{\boldsymbol{A}_c \tau} \boldsymbol{b}_c d\tau \\ \nu_k \le \mu_{(j-1)} : & 0 \end{cases}$$

$$0 = \mu_0 < \mu_1 < \mu_2 < \dots < \mu_N = 1, \qquad (8)$$

$$0 \le \nu_1 < \nu_2 < \dots < \nu_M < 1, \qquad (9)$$

where $\mu_j (j = 0, 1, \dots, N)$ and $\nu_k (k = 1, \dots, M)$ are the parameters for the multirate sampling as shown in Fig. 3. If T_f is divided at same intervals, $\mu_j = j/N, \nu_k = (k-1)/M$.

In the most simple case of $T_y = T_u$, μ_j is equal to ν_{k-1} and $\boldsymbol{P}[z]$ of (5) can be calculated more simply by

$$\left[\begin{array}{c|cccc} \boldsymbol{A}_s^n & \boldsymbol{A}_s^{n-1}\boldsymbol{b}_s & \boldsymbol{A}_s^{n-2}\boldsymbol{b}_s & \cdots & \boldsymbol{b}_s \\ \hline \boldsymbol{c}_s & d_s & 0 & \cdots & 0 \\ \boldsymbol{c}_s \boldsymbol{A}_s & \boldsymbol{c}_s \boldsymbol{b}_s & d_s & \cdots & 0 \\ \vdots & \vdots & & & \vdots \\ \boldsymbol{c}_s \boldsymbol{A}_s^{n-1} & \boldsymbol{c}_s \boldsymbol{A}_s^{n-2}\boldsymbol{b}_s & \boldsymbol{c}_s \boldsymbol{A}_s^{n-3}\boldsymbol{b}_s & \cdots & d_s \end{array} \right], (10)$$

where $P[z_s] = \{\boldsymbol{A}_s, \boldsymbol{b}_s, \boldsymbol{c}_s, d_s\}$ is the plant discretized by the zero-order-hold on $T_y(= T_u)$ and $z_s \triangleq e^{sT_y}$.

The proposed method employs the multirate-input control as the two-degree-of-freedom control, as shown in Fig. 1. In the figures, $\mathcal{H}_\mathcal{M}$ and $\mathcal{S}_\mathcal{M}$ represent the multirate hold and the multirate sampler respectively. The functions of $\mathcal{H}_\mathcal{M}$ and $\mathcal{S}_\mathcal{M}$ are shown in Fig. 3.

In the ideal tracking control system, the transfer characteristic (G_{yr}) from the command r to the output y is generally 1. In this paper, the feedforward controller $\boldsymbol{C}_1[z]$ is considered so that the transfer characteristic from the desired state $\boldsymbol{x}_d$ to the plant state $\boldsymbol{x}$ can be $\boldsymbol{I}$.

3.2 Design of the feedback controller $\boldsymbol{C}_2[z]$

Before the perfect tracking controller $\boldsymbol{C}_1[z]$ is designed, the feedback controller $\boldsymbol{C}_2[z]$ has to be determined. Here, the $\boldsymbol{C}_2[z]$ must be a robust controller which let the sensitivity function $\boldsymbol{S}[z] = (\boldsymbol{I} - \boldsymbol{P}[z]\boldsymbol{C}_2[z])^{-1}$ be small enough in the frequency of the desired trajectory. The reason is that the sensitivity function $\boldsymbol{S}[z]$ represents the variation of the command response $\boldsymbol{G}_{yr}[z]$ under the variation of $\boldsymbol{P}[z]$ [13].

First, for systems without special hardware restrictions, in which the feedback loop is single-rate ($T_y = T_u$), the feedback controller $C_2[z_s] = \{\boldsymbol{A}_s, \boldsymbol{b}_s, \boldsymbol{c}_s, d_s\}$ is designed for $P_c(s)$ on single-rate sampling period $T_y(= T_u)$, where $z_s = e^{sT_y}$. After that, $C_2[z_s]$ is
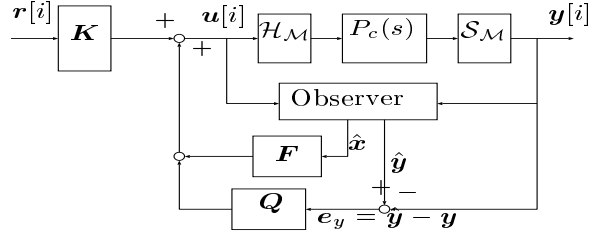
Figure 4. Basic structure of TDOF control.

transferred to n inputs n outputs system $\boldsymbol{C}_2[z]$ by (10) in order to realize $\boldsymbol{C}_1[z]$ and $\boldsymbol{C}_2[z]$ together, where $z = e^{sT_f} = z_s^n$ and $T_f = nT_y$.

Second, systems with special hardware restrictions are considered, in which the feedback-loop also may become multirate ($T_y < T_u$ or $T_y > T_u$). [10] and [14] proposed the multirate feedback controllers by the inter-sample observer and the sampled-data theory respectively. These multirate controllers may improve the feedback characteristics. However, the perfect tracking can be achieved, even if the single-rate feedback controller is simply designed on the longer period between T_y and T_u, and transferred to M inputs N outputs controller $\boldsymbol{C}_2[z]$ on T_f.

3.3 Design of the Perfect Tracking Controller $\boldsymbol{C}_1[z]$

In this section, the multirate feedforward controller $\boldsymbol{C}_1[z]$ is designed so that the perfect tracking can be assured at every sampling point T_r.

(3) can be transferred from the flame period T_f to the reference period $T_r = T_f/L$ by [1]

$$\tilde{\boldsymbol{x}}[i+1] = \tilde{\boldsymbol{A}}\boldsymbol{x}[i] + \tilde{\boldsymbol{B}}\boldsymbol{u}[i], \qquad (11)$$

where $q \triangleq 1/L = n/N$, and where matrices $\tilde{\boldsymbol{A}}, \tilde{\boldsymbol{B}}$ and vectors $\tilde{\boldsymbol{x}}$ are given by

$$\tilde{\boldsymbol{x}}[i+1] \triangleq \left[\begin{array}{c} \boldsymbol{x}[i+q] \\ \vdots \\ \boldsymbol{x}[i+lq] \\ \vdots \\ \boldsymbol{x}[i+1] \end{array} \right], \ \ \tilde{\boldsymbol{A}} \triangleq \left[\begin{array}{c} e^{\boldsymbol{A}_c T_r} \\ \vdots \\ e^{\boldsymbol{A}_c l T_r} \\ \vdots \\ e^{\boldsymbol{A}_c L T_r} \end{array} \right], \quad (12)$$

$$\tilde{\boldsymbol{B}} \triangleq \left[\begin{array}{cccccc} \boldsymbol{B}_L & \boldsymbol{O} & \cdots & \cdots & \cdots & \boldsymbol{O} \\ \vdots & \ddots & & & & \boldsymbol{O} \\ \boldsymbol{B}_{L-l} & \cdots & \boldsymbol{B}_L & \boldsymbol{O} & \cdots & \boldsymbol{O} \\ \vdots & & & \ddots & & \boldsymbol{O} \\ \boldsymbol{B}_1 & \boldsymbol{B}_2 & \cdots & \cdots & \cdots & \boldsymbol{B}_L \end{array} \right], \quad (13)$$

$$\boldsymbol{B}_l = [\boldsymbol{b}_{(l-1)n+1}, \cdots, \boldsymbol{b}_{ln}] \quad (l = 1, \cdots, L). \qquad (14)$$

---

[1]In case 1,(11) is equal to (3) ($\boldsymbol{x}[i+1] = \boldsymbol{A}\boldsymbol{x}[i] + \boldsymbol{B}\boldsymbol{u}[i]$), because of $L = 1$.
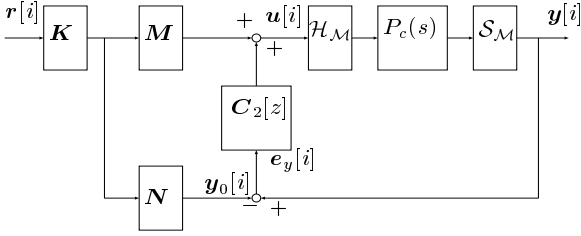
Figure 5. Implementation of the proposed controller.

From Fig. 1, the multirate control law of the proposed method is described by

$$u = C_1 r + C_2 y \tag{15}$$
$$= F\hat{x} + Q e_y + K r, \tag{16}$$

where $K, Q \in RH_\infty$ are free parameters. Therefore, Fig. 1 can be transferred to Fig. 4 [15]. In this paper, K becomes a constant matrix.

Because the estimation errors of the observer become zero ($\hat{x} = x, e_y = 0$) for the nominal plant, from (11) and (16), this system is represented by

$$\tilde{x}[i+1] = (\tilde{A} + \tilde{B}F)x[i] + \tilde{B}Kr[i]. \tag{17}$$

Because non-singularity of the matrix B can be assured by $T_r = nT_u$ [11], $\tilde{B}$ also becomes non-singular. Therefore, the parameters F and K can be selected so that following equations are satisfied.

$$\tilde{A} + \tilde{B}F = O \ , \quad \tilde{B}K = I \tag{18}$$

From (18), F, K are given by

$$F = -\tilde{B}^{-1}\tilde{A} \ , \quad K = \tilde{B}^{-1}. \tag{19}$$

Therefore, (17) is described by

$$\tilde{x}[i+1] = r[i]. \tag{20}$$

Utilizing the future desired state, let the reference input be

$$r[i] = \tilde{x}_d[i+1], \tag{21}$$

where $\tilde{x}_d[i]$ is desired state. From (20) and (21), we find the perfect tracking $\tilde{x}[i] = \tilde{x}_d[i]$ is achieved at every sampling point T_r.

Here, Fig. 1 can be represented by Fig. 5 because (15) is transferred to (22) [13]. Therefore, the proposed controller is simply implemented by (22).

$$u = (M - C_2 N)Kr + C_2 y \tag{22}$$

$$M = \left[\begin{array}{c|c} A + BF & B \\ \hline F & I \end{array}\right] = I + z^{-1}FB$$
$$N = \left[\begin{array}{c|c} A + BF & B \\ \hline C + DF & D \end{array}\right] = D + z^{-1}(C + DF)B, \tag{23}$$

where M and N are the parameters of the coprime factorization of the plant $P[z] = NM^{-1}$. The two-degree-of-freedom controller (22) should be realized in minimum order.

3.4 Structure of the Perfect Tracking Controller $C_1[z]$

In this section, it is shown that the structure of the perfect tracking controller is very simple and clear. From (19) and (23), two elements MK and NK in Fig. 5 are represented by

$$MK = (I - z^{-1}\tilde{B}^{-1}\tilde{A}B)\tilde{B}^{-1}, \tag{24}$$
$$NK = z^{-1}CB\tilde{B}^{-1} + D(I - z^{-1}\tilde{B}^{-1}\tilde{A}B)\tilde{B}^{-1}. \tag{25}$$

On the other hand, from (3) and (11), the transfer function from $u[i]$ to $\tilde{x}[i+1]$ is described by

$$\tilde{x}[i+1] = \left[\begin{array}{c|c} A & B \\ \hline A & B \end{array}\right] u[i]. \tag{26}$$

The inverse system of (26) is given by

$$u[i] = \left[\begin{array}{c|c} A - B\tilde{B}^{-1}\tilde{A} & B\tilde{B}^{-1} \\ \hline -\tilde{B}^{-1}\tilde{A} & \tilde{B}^{-1} \end{array}\right] \tilde{x}[i+1]. \tag{27}$$

From the definitions of $\tilde{A}$ and $\tilde{B}$ in (12), (13), the following equations are obtained.

$$A = \overbrace{[O, \cdots, O}^{L-1}, I]\tilde{A}, \tag{28}$$
$$B = [O, \cdots, O, I]\tilde{B}. \tag{29}$$

Thus, the $(1,1)$ element of the matrix (27) becomes

$$A - B\tilde{B}^{-1}\tilde{A} = A - [O, \cdots, O, I]\tilde{A} = O. \tag{30}$$

Therefore, (27) is given by [2]

$$u[i] = \left[\begin{array}{c|c} O & B\tilde{B}^{-1} \\ \hline -\tilde{B}^{-1}\tilde{A} & \tilde{B}^{-1} \end{array}\right] \tilde{x}[i+1]. \tag{31}$$

From (24) and (31), MK is equal to the transfer function from $\tilde{x}[i+1]$ to $u[i]$, and it represents the stable inverse system. This point is one of the advantages of the multirate control because the inverse system becomes unstable in the single-rate systems. Moreover, (4) is described from (31) by [3]

$$y[i] = z^{-1}Cx[i+1] + Du[i]$$
$$= z^{-1}C[O, \cdots, O, I]\tilde{x}[i+1]$$
$$\quad + D(I - z^{-1}\tilde{B}^{-1}\tilde{A}B)\tilde{B}^{-1}\tilde{x}[i+1] \tag{32}$$

From (25) and (32), it is shown that NK represents the transfer function from $\tilde{x}[i+1]$ to $y[i]$.

---

[2]In case 1, (32) becomes $y[i] = z^{-1}Cx[i+1]$, because of $D = O$.

[3]In case 1, (31) becomes $u[i] = B^{-1}(I - z^{-1}A) x[i+1]$, which is directly obtained from $x[i+1] = Ax[i] + Bu[i]$ of (3), because of $\tilde{B} = B$.
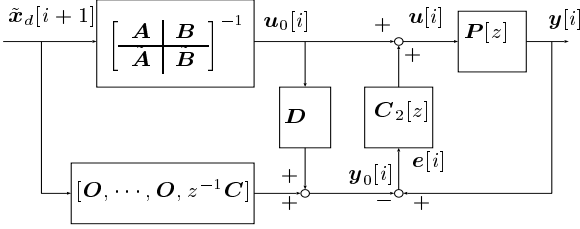
Figure 6. Structure of the proposed controller.

As a result, the structure of the proposed controller is shown in Fig. 6. The plant $P[z]$ is driven by the stable inverse system. When the tracking error e is generated by disturbance or modeling error, the robust feedback controller $C_2[z]$ works in order to eliminate e.

4   Illustrative Examples

In this section, the simulation and experimental results for the position tracking control system of the dc servo motor are presented, and the advantages of the proposed approach are demonstrated.

4.1   Case 1 on $T_y = T_u$

First, an most simple example of $T_y = T_u$ (case 1) is considered. The dc servo motor with current control is described by

$$P_c(s) = \frac{K}{Js^2}. \tag{33}$$

The feedback controller $C_2[z]$ is obtained from the H_∞ mixed-sensitivity problem, which includes an integrator and becomes 3rd order [16]. Calculating (22) and minimally realizing the obtained $C_1[z]$ and $C_2[z]$, the controller $[C_1, C_2]$ becomes 5th order system.

Simulation and experimental results under the sinusoidal desired trajectories of period $\omega_{ref} = 25$[rad/s] are shown in Fig. 7. In this system, both input and output periods are $T_y = T_u = 1$[ms]. Because this plant is 2nd order system, the sampling period of the reference signal becomes $T_r = 2$[ms] ($N = 2$).

In the following simulations and experiment, the proposed method is compared with both SPZC and ZPETC proposed by [1] at same T_y and T_u. Therefore, the reference sampling period T_r of the proposed method is twice as long as those of SPZC and ZPETC, because these methods are single-rate approaches and sampling periods are set to $T_y = T_u = T_r = 1$[ms]. However, the proposed controller utilizes the desired trajectories of position and velocity, although SPZC and ZPETC use those of only position.

(a) Position (Sim.)   (b) Error (Sim.)

(c) Input (Sim.)   (d) Position (Exp.)
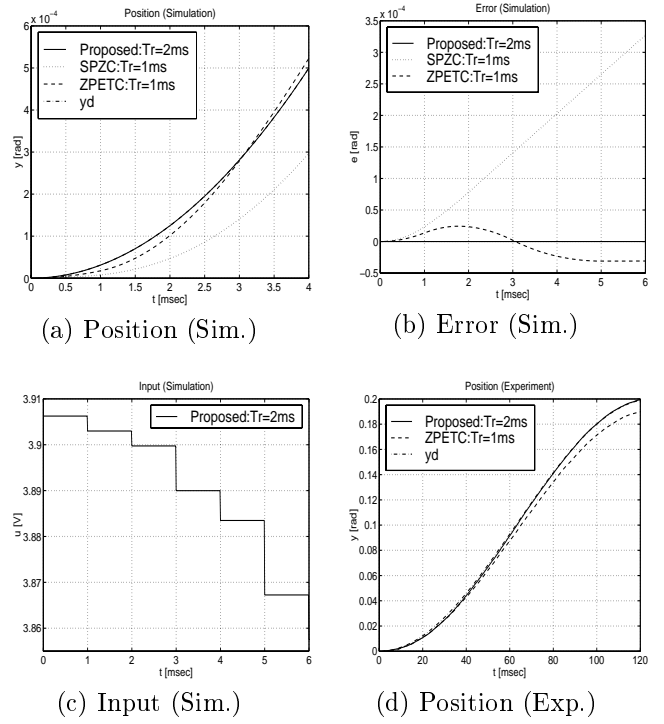
Figure 7.   Simulation and Experimental Results ($T_y = T_u = 1$[ms], $T_r = 2$[ms], $\omega_{ref} = 25$[rad/s])
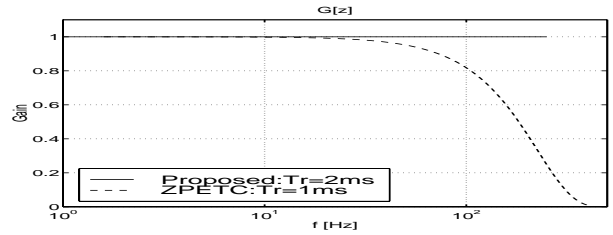
Figure 8. Frequency response $y[z]/y_d[z]$

Fig. 7(a)(b) show that the proposed method gives better performance both than the SPZC and the ZPETC. While the responses of the SPZC and ZPETC have large tracking errors caused by the unstable zero, those of the proposed method have zero tracking errors. The simulated time response of the control input is shown in Fig. 7(c), which indicates that the control input of the proposed method is smooth in spite of using the multirate input control. Thus, we find the proposed multirate feedforward method is very practical. Moreover, the experimental result also indicates that the proposed method has high tracking performance as shown in Fig. 7(d). Furthermore, Fig. 7(a)(b) also show that the inter-sample responses are very smooth because not only position but also velocity follow the desired trajectories at every sampling point T_r.

The frequency responses from the desired trajectory $y_d[i]$ to the output $y[i]$ are shown in Fig. 8. Because the proposed method assures the perfect
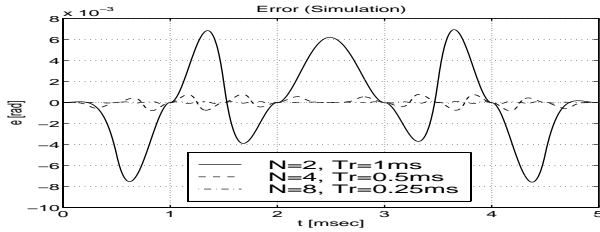
Figure 9. Simulation results ($T_y = 1$[ms], $T_u = T_y/N, T_r = 2T_y/N$, $\omega_{ref} = 1250$[rad/s]).

tracking, the command response becomes 1 in the all frequency. However, the gain of ZPETC decreases in the high frequency.

This example indicates that the proposed multirate feedforward controller has higher tracking performance than the single-rate controller even in the usual servo system ($T_y = T_u$) without special hardware restrictions.

4.2   Case 2 on $T_u = T_y/N$

Second, it is assumed that the output sampling period is restricted to $T_y = 1$[ms] by hardware, and the control input can be changed more frequently ($T_u = T_y/N$). In this case, the perfect tracking is guaranteed at $L(= N/n = N/2)$ times during T_y. The single-rate feedback controller is designed on 1[ms] period.

While the desired trajectories were slow in Fig. 7 ($\omega_{ref} = 25$[rad/s]), Fig. 9 shows the simulated tracking error for faster trajectories ($\omega_{ref} = 1250$[rad/s]). Compared with $N = 2$, the tracking performances are improved for large input multiplicity $N = 4$ and 8, because the perfect tracking is assured at $L(= N/2)$ inter-sample points. In [10], this approach is applied to the seeking control of hard disk drive.

5   Conclusion

A novel perfect tracking control method in use of the multirate feedforward control was proposed. The proposed method was extended to be applicable to various systems with hardware restrictions both on the sampling periods and control periods. Moreover, it is shown that the structure of the proposed perfect tracking controller is very simple and clear.

Furthermore, two illustrative examples of position control using a dc servo motor are performed, and the advantages of this approach are demonstrated by the simulations and experiments. First example illustrates the proposed multirate controller has higher performance than the conventional single-rate controller even in the usual system ($T_y = T_u$) without special hardware restrictions. Second example also indicates that the inter-sample response is improved

by multirate feedforward control for the system with longer sampling period ($T_y > T_u$).

References

[1] M. Tomizuka: "Zero phase error tracking algorithm for digital control", ASME, J. Dynam. Syst., Measur., and Contr., **109**, pp. 65–68 (1987).

[2] K. J. Åström, P. Hangander and J. Sternby: "Zeros of sampled system", Automatica, **20**, 1, pp. 31–38 (1984).

[3] B. Haack and M. Tomizuka: "The effect of adding zeros to feedforward controllers", ASME, J. Dynam. Syst., Measur., and Contr., **113**, pp. 6–10 (1991).

[4] D. Torfs, J. D. Schutter and J. Swevers: "Extended bandwidth zero phase error tracking control of nonminimal phase systems", ASME, J. Dynam. Syst., Measur., and Contr., **114**, pp. 347–351 (1992).

[5] E. Gross, M. Tomizuka and W. Messner: "Cancellation of discrete time unstable zeros by feedforward control", ASME, J. Dynam. Syst., Measur., and Contr., **116**, pp. 33–38 (1994).

[6] H. Fujimoto and A. Kawamura: "Perfect tracking digital motion control based on two-degree-of-freedom multirate feedforward control", IEEE Int. Workshop Advanced Motion Control, pp. 322–327 (1998).

[7] P. T. Kabamba: "Control of linear systems using generalized sampled-data hold functions", IEEE Trans. Automat. Contr., **32**, 9, pp. 772–783 (1987).

[8] T. Mita, Y. Chida, Y. Kazu and H. Numasato: "Two-delay robust digital control and its applications – avoiding the problem on unstable limiting zeros", IEEE Trans. AC, **35**, 8, pp. 962–970 (1990).

[9] K. L. Moore, S. P. Bhattacharyya and M. Dahleh: "Capabilities and limitations of multirate control schemes", Automatica, **29**, 4, pp. 941–951 (1993).

[10] H. Fujimoto, Y. Hori, T. Yamaguchi and S. Nakagawa: "Proposal of perfect tracking and perfect disturbance rejection control by multirate sampling and applications to hard disk drive control", Conf. Decision Contr., pp. 5277–5282 (1999).

[11] M. Araki: "Recent developments in digital control theory", 12th IFAC World Congress, Vol. 9, pp. 251–260 (1993).

[12] H. Fujimoto, A. Kawamura and M. Tomizuka: "Generalized digital redesign method for linear feedback system based on N-delay control", IEEE/ASME Trans. Mechatronics, **4**, 2, pp. 101–109 (1999).

[13] T. Sugie and T. Yoshikawa: "General solution of robust tracking problem in two-degree-of-freedom control systems", IEEE Trans. Automat. Contr., **31**, 6, pp. 552–554 (1986).

[14] T. Chen and L. Qiu: "H_∞ design of general multirate sampled-data control systems", Automatica, **30**, 7, pp. 1139–1152 (1994).

[15] K. Zhou, J. Doyle and K. Glover: "Robust and Optimal Control", Prentice-Hall, Inc (1996).

[16] T. Mita, M. Hirata and S. B. Villas: "H_∞ servo controller design for plants having poles on the $j\omega$ axis", Conf. Decision Contr., pp. 2568–2573 (1995).